

# CAV2021

11<sup>th</sup> International Symposium on Cavitation  
May 10-13, 2021, Daejeon, Korea

## Numerical simulation of a water cavitation jet peening

Zhaofeng Han <sup>1,2\*</sup>, Thibaut Chaise <sup>1</sup>, Cyril Mauger <sup>2</sup>, Thomas Elguedj <sup>1</sup>, Nicolas Boisson <sup>1</sup> and Mahmoud El Hajem <sup>2</sup>

<sup>1</sup>Univ Lyon, INSA Lyon, CNRS UMR5259, LaMCoS, F-69621, France

<sup>2</sup>Univ Lyon, INSA Lyon, École Centrale de Lyon, Université Claude Bernard Lyon I, CNRS, LMFA, UMR 5509, F-69621, VILLEURBANNE, France

**Abstract:** Shot peening is commonly used as an effective method to extend the service life of parts and reduce the residual tensile stresses. The main principle of this surface treatment method is to introduce compressive residual stresses into parts, thereby preventing the crack-propagation. Water cavitation peening (WCP) is a recent technology that allows generating high-intensity pressure waves and micro-jet at the surface of parts via a cavitating jet. However, it is a challenge to predict the pressure intensity at the treatment surface and therefore being able to make predictive modelization of the process. To anticipate the pressure distribution around the cavitating jet, a multiple steps approach has been developed. First, through the study of a single cavitation bubble, understand the pressure pulse generated by a single bubble during its collapse process. The second step is to establish a numerical simulation of the cavitating jet near the nozzle with ANSYS Fluent. Accordingly, the cavitation area and the vapor volume fraction at different section of cavitating jet will be predicted. Then, the mechanical loading at the surface of parts will be defined by these sources. The second part of the approach is here studied. The simulation results will be compared with experimental high-speed camera imaging of the cavitating jet.

**Keywords:** Surface treatment, water cavitation peening, cavitating jet, numerical simulation.

### 1. Introduction

Shot peening is a surface treatment process that reduces residual stresses from the manufacturing of a part by applying compressive residual stressed on the surface. This process delays the propagation of cracks and increases the corrosion resistance and service life of the part [1–3]. Conventional shot peening consists in projecting shots onto the surface of the part. Therefore, it can contaminate the surface of the part and its environment during processing. For some parts with complex geometry, conventional shot peening does not allow to reach all surfaces. To overcome these problems, water cavitation peening (WCP) [4,5] has been developed. The part to be treated is placed in an enclosure filled with water. A high-speed water jet send to the part. The velocity difference between the surrounding water and the jet induces significant shear stresses which will give rise to the appearance of strongly vortex structures, and produce a low-pressure area [6]. Moreover, cavitation bubble clouds can be generated in the low-pressure area. The simulation of the submerged water jet is an important step to anticipate the pressure distribution generated by the cavitation jet [7].

The cavitation peening process can be simulated macroscopically. This study uses ANSYS Fluent to achieve the simulation. For cavitation flow, it is composed by water and vapor, in the process of cavitation, the two phases will also be accompanied by mass transfer. In this simulation, the mixture model [8] has been used for multiphase flow, the realizable k- $\epsilon$  model [9] simulates the turbulence and the Singhal et al.

\* Corresponding Author: zhaofeng.han@insa-lyon.fr

model [10] (also called full cavitation model) simulates the mass transfer by cavitation between the water and the vapor. In addition, it is assumed that between the two phases and at the inner wall of nozzle a no-slip condition is satisfied.

**2. Model establishment**

Figure 1 describes the geometry of the simulated nozzle. Due to the axis-symmetry of the considered problem, only a slice of the model is shown. This geometry of the nozzle is obtained by high-precision measurement of the real nozzle used in the experiment. In order to optimize the calculation time, full-scale modeling of the water tank is not performed here. After studying the convergence of the computational domain in detail, we chose to model an area of 50 × 10 mm in size. The red border in the left of Figure 1 is the inlet of the system. The boundary condition here is a pressure-inlet, according to the actual pressure of the experiments, the pressure inlet is 30 MPa. In addition, the blue boundary represents the environmental pressure expressed as a pressure-outlet with a value of 0 MPa. The inner wall of the nozzle, represented in green in Fig. 1, satisfies the no-slip boundary condition and the outer wall of nozzle, in black, satisfies the slip boundary condition. The orange boundary in Fig. 1 corresponds to the condition of axis-symmetry. ANSYS-ICEM has been used to create computational domains and structured grids. Finally, the entire computational domain is divided into 197 040 uniformly structured 2D dimensional grids with a maximum size of 50 μm × 50 μm. In this simulation, the turbulence intensity is 5% for both pressure-inlet and pressure-outlet.

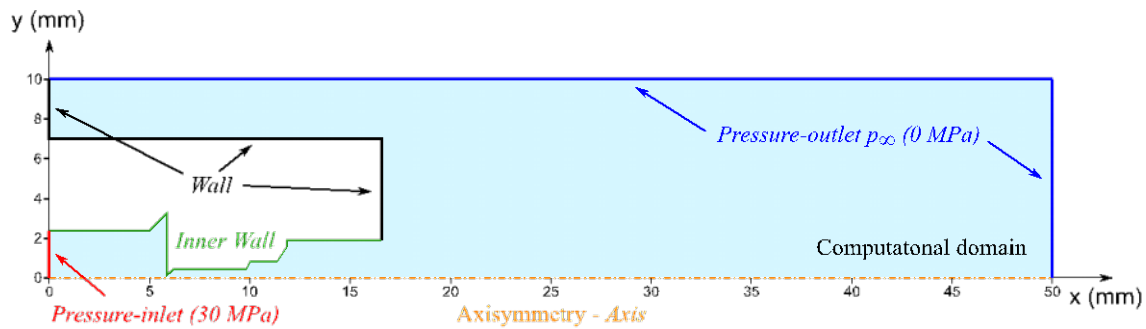


**Figure 1.** Schematic representation of the model geometry used to simulate cavitation jet. The inner wall (green border) hypothesis satisfies the no-slip boundary condition and the outer wall (black border) satisfies the slip boundary condition.

**3. Numerical simulation results and analyses**

The establishment of the cavitation flow is divided into two steps here. The first step is to solve the mixture model and the realizable k-ε model to obtain a jet flow without cavitation used as the initial stage. After it is stabilised, the full cavitation model (Singhal et al. [10]) is added to simulate the cavitation phenomenon and start the transient calculation. Figure 2 shows the velocity distribution of the underwater water jet in contour map and the vorticity magnitude in path-line diagram at 5.65 ms. It can be seen that due to the sudden reduction in the diameter of the nozzle, the water flow is accelerated rapidly under the pressure, and will reach a maximum speed of 246 m/s inside the nozzle. When the water flow sprays out of the nozzle, under the double action of inertial forces and pressure, the water flow will continue to rush forward. However, the still water in the surrounding environment will have a certain resistance to the

\* Corresponding Author: zhaofeng.han@insa-lyon.fr

water jet, thus preventing the water flux from continuing to move, and a huge shear force is generated at the contact surface of the water jet and the environmental fluid.

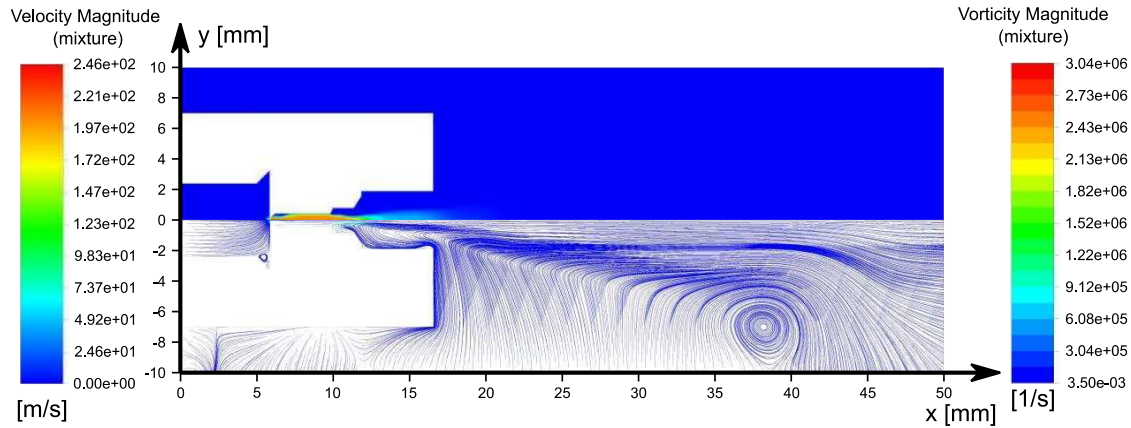


**Figure 2.** The upper half of the image is the velocity distribution represented by the contour map and the vorticity magnitude is represented by the path-line diagram in the lower part at 5.65 ms.

In addition to the velocity distribution, the distribution of vapor volume fraction is also studied. Figure 3 shows the distribution of vapor volume fraction at 5.65 ms. For the cavitation inside the nozzle, the high-speed water jet located in the center of the nozzle and the boundary layer of the nozzle generate a huge shear force, and a small range of vortices are generated at the wall of the beginning of the nozzle. This process is accompanied by the generation of a large number of cavitation bubble and these bubble cores will expand and accumulate rapidly, thereby forming cavitation bubble cloud, the maximum volume fraction of vapor reaches 100 %. In the expansion area of the nozzle outlet, there will be a back flow near the inner wall of the nozzle, and under the impact of the high-speed cavitation flow, a second low pressure zone appears due to the strong shear force between the back flow and the cavitation flow. This process will be amplified to a certain extent cavitation area. After that, the volume fraction of vapor gradually decreases with the flow of the water jet, and disappears quickly at the nozzle outlet. For more detail of cavitation jet, Figure 4 (a) shows the curve of vapor volume fraction on the axis of symmetry. To understand the fluctuation of cavitation flow, four characteristic surfaces were added to the model, and the physical parameters on the 4 surfaces were tracked over time. The 4 surfaces are the nozzle “throat”, the center of nozzle, nozzle outlet and the center of water tank. The average value of vapor volume fraction of these 4 surfaces over time has been shown in Fig. 4 (b), the average fluctuation period is 0.43 ms. This period will be compared with experimental data in the future.

In the experiment, we can only observe the presence or absence of cavitation areas through high-speed cameras, so it is difficult to determine the cavitation areas by the volume fraction of vapor. On the experimental images, the light rays are diffracted by the liquid-vapor interface, which leads to shadow areas on the camera sensor. Even for very low vapor volume fractions, this diffract phenomenon still produces. In order to facilitate the comparison with the experimental data in the future, the area with the vapor volume fraction of 3%, 4% and 5% is marked in the form of white contour lines in Fig. 3. In this study, 5% vapor volume fraction is regarded as the visible cavitation area in the experiment, so the length of cavitation jet (from nozzle outlet to contour line of 5%) is about 5 mm in this simulation.

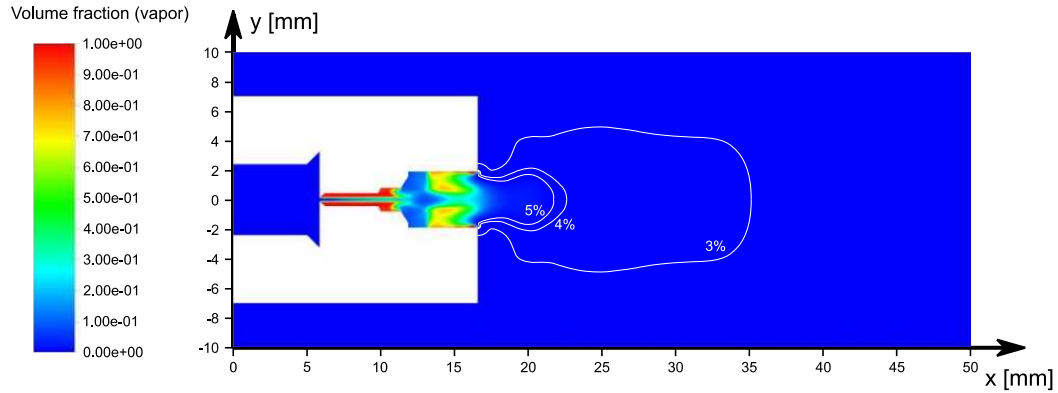


**Figure 3.** Distribution of volume fraction of vapor at 5.65 ms. The white contour lines from outside to inside represent the contours with volume fraction of vapor 3%, 4% and 5% respectively.

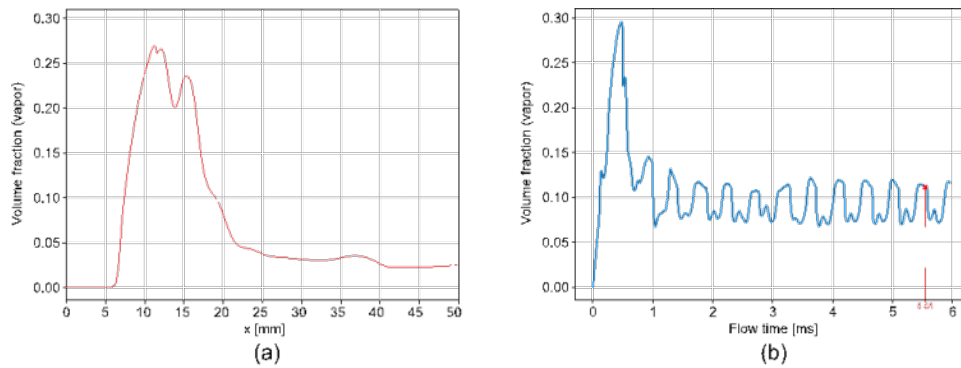


**Figure 4.** (a) Distribution curve of volume fraction of vapor on the axis of symmetry at 5.65 ms; (b) The curve of the average value of vapor volume fraction on the characteristic surface over time. The average fluctuation period is 0.43 ms.

#### 4. Conclusions

A model of cavitating jet with a geometry of real nozzle structure is established. The distribution of velocity, vorticity, the volume fraction of vapor inside and near the nozzle and the fluctuation of cavitation flow has been analyzed in detail. The average fluctuation period is 0.43 ms, and the length of cavitation jet with 5 % vapor volume fraction is about 5 mm. The current results show the potential of predicting the cavitation area and then predict the pressure of the cavitating jet through the model.

In the future, the results of numerical simulation will be compared with experimental results to verify the accuracy of the model.

**Acknowledgments:** This work was supported by the project MoCaPee of the Institut Carnot Ingénierie@Lyon.

# CAV2021

11<sup>th</sup> International Symposium on Cavitation  
May 10-13, 2021, Daejeon, Korea

## References

1. G. H. Farrahi, J. L. Lebrun, and D. Couratin. Effect of shot peening on residual stress and fatigue life of a spring steel. *Fatigue & Fracture of Engineering Materials & Structures*, vol. 18, 1995, p. 211-220.
2. M. A. S. Torres, H. J. C. Voorwald. An evaluation of shot peening, residual stress and stress relaxation on the fatigue life of AISI 4340 steel. *International Journal of fatigue*. 24 (2002) 877-886.
3. J. Tirosh. Extended fatigue life by shot peening process via shakedown analysis. *Journal of Applied Mechanics*, vol. 75, 2008.
4. H. Soyama, Y. Yamauchi, Y. Adachi, K. Sato, T. Shindo, and R. Oba. High-speed observations of the cavitation cloud around a high-speed submerged water jet. *JSME International Journal Series B Fluids and Thermal Engineering*, 38(2) :245-251, 1995.
5. H. Soyama, J. D. Park, M. Saka. Use of Cavitating jet for Introducing Compressive Residual Stress, vol, 122, 2000.
6. A. Sou, B. Bicer, A. Tomiyama. Numerical simulation of incipient cavitation flow in a nozzle of fuel injector. *Computers & Fluids*, vol. 103, 2014, p. 42-48.
7. E. Sonde, T. Chaise, N. Boisson, D. Nelias. Modeling of cavitation peening : Jet, bubble growth and collapse, micro-jet and residual stresses. *Journal of Materials Processing Technology*. 262(2018) 479-491.
8. R. M. Bowen. Theory of Mixtures. In A. C. Eringen, editor *Continuum Physics*. Academic Press, New York. 1-127. 1976.
9. T. H. Shih, W. W. Liou, A. Shabbir, Z. Yang, and J. Zhu. A new k-  $\epsilon$  Eddy-Viscosity Model for high Reynolds Number Turbulent Flow – Model Development and Validation. *Computer Fluids*. 24(3). 227-238. 1995.
10. A. K. Singhal, M. M. Athavale, H. Li and Y. Jiang. Mathematical basis and validation of the full cavitation model. *J. Fluids Eng.*, 124(3):617-624, 2002.